






Speech Enhancement and Dereverberation with Diffusion-based Generative Models

Julius Richter , *Student Member, IEEE*, Simon Welker , *Student Member, IEEE*, Jean-Marie Lemerrier , *Student Member, IEEE*, Bunlong Lay , Timo Gerkmann , *Senior Member, IEEE*

Abstract—Recently, diffusion-based generative models have been introduced to the task of speech enhancement. The corruption of clean speech is modeled as a fixed forward process in which increasing amounts of noise are gradually added. By learning to reverse this process in an iterative fashion conditioned on the noisy input, clean speech is generated. We build upon our previous work and derive the training task within the formalism of stochastic differential equations. We present a detailed theoretical review of the underlying score matching objective and explore different sampler configurations for solving the reverse process at test time. By using a sophisticated network architecture from natural image generation literature, we significantly improve performance compared to our previous publication. We also show that we can compete with recent discriminative models and achieve better generalization when evaluating on a different corpus than used for training. We complement the evaluation results with a subjective listening test, in which our proposed method is rated best. Furthermore, we show that the proposed method achieves remarkable state-of-the-art performance in single-channel speech dereverberation. Our code and audio examples are available online¹.

Index Terms—speech enhancement, speech dereverberation, diffusion models, score-based generative models, stochastic differential equations, score matching.

I. INTRODUCTION

SPEECH enhancement aims to recover clean speech signals from audio recordings that are impacted by acoustic noise or reverberation [1]. To this end, computational approaches often exploit the different statistical properties of the target and interference signals [2]. Machine learning algorithms can be used to extract these statistical properties by learning useful representations from large datasets. A wide class of methods employed for speech enhancement are discriminative models that learn to directly map noisy speech to the corresponding clean speech target [3]. Common approaches include time-frequency (T-F) masking [4], spectral mapping [5], or operating directly in the time domain [6]. These supervised

methods are trained with a variety of clean/noisy speech pairs containing multiple speakers, different noise types, and a large range of signal-to-noise ratios (SNRs). However, it is nearly impossible to cover all possible acoustic conditions in the training data to guarantee generalization. Furthermore, some discriminative approaches have been shown to result in unpleasant speech distortions that outweigh the benefits of noise reduction [7].

The use of generative models for speech enhancement, on the other hand, follows a different paradigm, namely to learn a prior distribution over clean speech data. Thus, they aim at learning the inherent properties of speech, such as its spectral and temporal structure. This prior knowledge can be used to make inferences about clean speech given noisy or reverberant input signals that are assumed to lie outside the learned distribution. Several approaches follow this idea and utilized deep generative models for speech enhancement [8]–[17]. Among them are methods that employ likelihood-based models for explicit density estimation such as the variational autoencoder (VAE) [18], or leverage generative adversarial networks (GANs) [19] for implicit density estimation. Bando et al. propose a statistical framework using a VAE trained in an unsupervised fashion to learn a prior distribution over clean speech [9]. At test time they combine the speech model with a low-rank noise model to infer the signal variances of speech and noise to build a Wiener filter for denoising. However, since the VAE is trained with clean speech only, the inference model (i.e. the encoder) that predicts the latent variable remains sensitive to noise. This has been shown to cause the generative speech enhancement method to produce speech-like sounds although only noise is present [9]. To mitigate this, it has been proposed to make the inference model robust to noisy speech by training on labeled data in a supervised manner [14], [15], or by disentangling the latent variable from high level information such as speech activity which can be estimated by supervised classifiers [12], [13]. Nevertheless, VAE-based speech enhancement methods remain limited due to the dimensionality reduction in the latent layer and the combined use of a linear noise model based on non-negative matrix factorization [9]–[15].

More recently, a new class of generative models, called diffusion-based generative models, has been introduced to the task of speech enhancement [20]–[23]. Diffusion-based generative models, or simply *diffusion models*, are inspired by non-equilibrium thermodynamics and exist in several variants [24]–[26]. All of them share the idea to gradually turn data into noise, and to train a neural network that learns to

This work has been funded by the German Research Foundation (DFG) in the transregio project Crossmodal Learning (TRR 169), DASHH (Data Science in Hamburg - HELMHOLTZ Graduate School for the Structure of Matter) with the Grant-No. HIDSS-0002, and the Federal Ministry for Economic Affairs and Climate Action, project 01MK20012S, AP380.

Simon Welker is with the Signal Processing Group, Department of Informatics, Universität Hamburg, 22527 Hamburg Germany, and with the Center for Free-Electron Laser Science, DESY, 22607 Hamburg, Germany (e-mail: simon.welker@uni-hamburg.de).

The other authors are all with the Signal Processing Group, Department of Informatics, Universität Hamburg, 22527 Hamburg Germany (e-mail: {julius.richter; jeanmarie.lemerrier; bunlong.lay; timo.gerkmann}@uni-hamburg.de).

¹<https://uhh.de/inf-sp-sgmse>

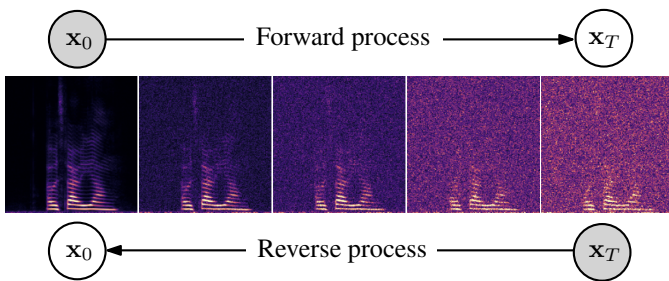


Fig. 1: Diffusion process on a spectrogram: In the forward process noise is gradually added to the clean speech spectrogram x_0 , while the reverse process learns to generate clean speech in an iterative fashion starting from the corrupted signal x_T .

invert this process for different noise scales. More specifically, the inference model is a fixed Markov chain, that slowly transforms the data into a tractable prior, such as the standard normal distribution. The generative model is another Markov chain that is trained to revert this process iteratively [25]. Therefore, diffusion models can be considered as deep latent variable models and have similar properties to VAEs, with the crucial difference that the inference model is not trained and that the latent variables have the same dimensionality as the input. This has the advantage to not rely on surrogate objectives to approximate maximum likelihood training such as the evidence lower bound, and enforces no strong restrictions on the model architecture. Recently, diffusion models have been connected with score matching [27] by looking at the stochastic differential equation (SDE) associated with the discrete-time Markov chain [28]. The forward process can be inverted, resulting in a corresponding reverse SDE which depends only on the score function of the perturbed data [29]. Using this continuous-time SDE formalism creates the opportunity to design novel diffusion processes that support the underlying generation task. In contrast to discrete Markov chains, it also allows the use of general-purpose SDE solvers to numerically integrate the reverse process for sampling.

Concerning the application of diffusion models for speech enhancement, there exist currently two approaches that differ conceptually in how the diffusion process is used. One approach is based on speech re-generation, i.e. a diffusion-based vocoder network is used to synthesize clean speech by sampling from an unconditional prior, while a conditioner network takes noisy speech as input and performs the core part of denoising by providing enhanced speech representations to the vocoder network [23], [30]. An auxiliary loss is introduced for the conditioner network to facilitate its ability to estimate clean speech representations [23]. The second approach, on the other hand, does not require any auxiliary loss and is not using two separate models for generation and denoising. Instead, it models the corruption of clean speech by environmental background noise or reverberation directly within the forward diffusion process, so that reversing this process would consequently result in generating clean speech. This has been proposed as a discrete diffusion process for time-domain speech signals [21], and as a continuous SDE-based diffusion process in the complex spectrogram domain

[22]. Interestingly, the original denoising score matching objective [31], which is to estimate the white Gaussian noise in the perturbed data, is essentially reminiscent of the goal of speech enhancement, which is to remove interfering noise or reverberation from speech signals. However, under realistic conditions the environmental noise or reverberation may not match the Gaussian assumption. Therefore, it was proposed to include real noise recordings in the diffusion process, either by linearly interpolating between clean and noisy speech along the process [21], or by defining such a transformation within the drift term of an SDE [22]. Note, however, that diffusion-based speech enhancement methods, unlike the VAE-based method described above, are not counted as unsupervised methods, since labeled data is used for training. Nevertheless, the learning objective remains generative in nature which is to learn a prior for clean speech per se rather than a direct mapping from noisy to clean speech. In fact, supervision is only exploited to learn the conditional generation of clean speech when noisy speech is given. Thus, current diffusion-based models for speech enhancement can be considered as conditional generative models trained in a supervised manner.

In this work, we build upon our previous method which defines the diffusion process in the complex spectral domain [22]. We present a detailed theoretical review of the underlying score-based generative model and propose a diffusion process which is defined as the solution of an Ornstein-Uhlenbeck SDE. The diffusion process is parameterized so that the added white Gaussian noise sufficiently masks the ambient noise, but still preserves high-level information about the structure of the speech, which serves as a guide in the reverse process. By using an architecture developed in the image processing community, we can significantly improve performance in comparison to our previous model. Interestingly, we also show that the approach achieves remarkable state-of-the-art performance in single-channel dereverberation tasks.

II. METHODS

A. Stochastic process

In this section, we motivate and describe in detail the stochastic process used in this work, as proposed in our previous publication [22]. The tasks at hand—speech enhancement and speech dereverberation—can be considered as conditional generation tasks: Given the noisy/reverberant speech, generate clean speech by using a generative model. Most previously published diffusion-based generative models are adapted to such conditional tasks either through explicit conditioning channels added to the deep neural network (DNN) [32], [33], or through combining an unconditionally trained score model with a separate model (such as a classifier) that provides conditioning in the form of a gradient [28], [34]. With our method, we explore a third possibility, which is to incorporate the particular task directly into the forward and reverse processes of a diffusion-based generative model.

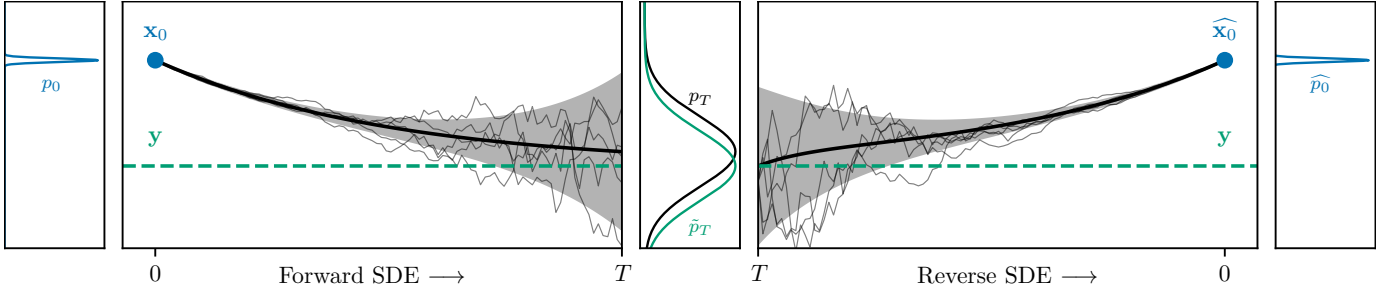


Fig. 2: The forward and reverse process illustrated with a single scalar variable. The mean (thick black line) of the forward process exponentially decays from clean speech \mathbf{x}_0 (blue) towards corrupted speech \mathbf{y} (green), and the standard deviation (shaded gray region) increases exponentially. The reverse process moves back to \mathbf{x}_0 , starting from a slightly mismatched distribution \hat{p}_T which is centered around \mathbf{y} rather than \mathbf{x}_T . Sample paths from both processes are shown as thin black lines.

We follow this idea by designing a stochastic diffusion process $\{\mathbf{x}_t\}_{t=0}^T$ modeled as the solution to a linear SDE,

$$d\mathbf{x}_t = \underbrace{\gamma(\mathbf{y} - \mathbf{x}_t)}_{:= \mathbf{f}(\mathbf{x}_t, \mathbf{y})} dt + \underbrace{\left[\sigma_{\min} \left(\frac{\sigma_{\max}}{\sigma_{\min}} \right)^t \sqrt{2 \log \left(\frac{\sigma_{\max}}{\sigma_{\min}} \right)} \right]}_{:= g(t)} d\mathbf{w}, \quad (1)$$

where \mathbf{x}_t is the current state of the process indexed by a continuous time variable $t \in [0, T]$ with the initial condition \mathbf{x}_0 representing clean speech, \mathbf{y} is the noisy or reverberant speech, and \mathbf{w} denotes a standard Wiener process. All variables in bold are assumed to be vectors in \mathbb{C}^d containing the coefficients of a complex spectrogram, whereas variables in regular font represent real scalar values. The vector-valued function $\mathbf{f}(\mathbf{x}_t, \mathbf{y})$ is referred to as the *drift* coefficient, while $g(t)$ is called the *diffusion* coefficient of \mathbf{x}_t . The parameter γ is a constant called *stiffness*, and σ_{\min} and σ_{\max} are constant parameters controlling the amount of Gaussian white noise injected at each timestep of the process.

From Eq. (1) it can be seen that the drift is purely deterministic, while the diffusion coefficient controls a random Wiener process. Note that we choose the diffusion coefficient identical to that of the so-called *Variance Exploding SDE* from Song et al. [28]. Our novel contribution lies in the added drift term, by which the intended task adaptation is achieved. Disregarding the stochastic diffusion term, i.e. by looking at the corresponding ordinary differential equation (ODE), the process can be thought of as an exponential decay from \mathbf{x}_0 to \mathbf{y} . By solving the associated reverse process, we move from \mathbf{y} to \mathbf{x}_0 and thus solve the target task of speech enhancement or dereverberation.

Following Anderson [29] and Song et al. [28], the SDE in Eq. (1) has an associated *reverse SDE*,

$$d\mathbf{x}_t = [-\mathbf{f}(\mathbf{x}_t, \mathbf{y}) + g(t)^2 \nabla_{\mathbf{x}_t} \log p_t(\mathbf{x}_t)] dt + g(t) d\bar{\mathbf{w}}, \quad (2)$$

where the *score* $\nabla_{\mathbf{x}_t} \log p_t(\mathbf{x}_t)$ is the term to be approximated by a DNN which is therefore called a *score model*. We denote the score model as $\mathbf{s}_\theta(\mathbf{x}_t, \mathbf{y}, t)$, which is parameterized by a set of DNN parameters θ and receives the current state of the process \mathbf{x}_t , the noisy speech \mathbf{y} , and the current time-step t as an input. Finally, by substituting the score model into the

reverse SDE in Eq. (2), we obtain the so-called *plug-in reverse SDE* [35],

$$d\mathbf{x}_t = [-\mathbf{f}(\mathbf{x}_t, \mathbf{y}) + g(t)^2 \mathbf{s}_\theta(\mathbf{x}_t, \mathbf{y}, t)] dt + g(t) d\bar{\mathbf{w}}, \quad (3)$$

which can be solved by various solver procedures, to be discussed in detail in Sec. II-C.

When considering the time evolution of the probability density function p_t of the process state \mathbf{x}_t , it can be thought of as a continuum of distributions $\{p_t\}_{t \in [0, T]}$ which is determined by the drift and the diffusion coefficient defined in Eq. (1). In Fig. 2, we illustrate this time evolution for a one-dimensional case and simulate five sample paths from the process. In the reverse process, the DNN has the task of learning this continuous family of distributions starting from p_T . Due to the exponential increase of the diffusion coefficient in the forward process with the initial condition $g(0) \approx 0$, the distribution p_0 essentially corresponds to the clean speech distribution, whereas the terminating distribution p_T is a strongly corrupted version of the noisy speech distribution. The particular characteristics in each noisy speech sample are strongly masked by the Gaussian white noise at $t = T$. Therefore, by learning the reverse process, the generative model learns a strong prior p_0 on clean speech, whereas the forward process terminates in a strongly corrupted distribution of the noisy speech, used as a weakly informative prior for generation. This overall idea is illustrated in Fig. 2. All sample paths of the forward process start exactly at x_0 , but exhibit starkly different trajectories at large t . The reverse process should then turn a high-variance sample x_T back into a low-variance estimate of x_0 .

B. Training objective

Next, we derive the objective function used for training the score model \mathbf{s}_θ . Since the SDE in Eq. (1) describes a Gaussian process, the mean and variance of the process state \mathbf{x}_t can be derived when its initial conditions are known [36]. This allows for direct sampling of \mathbf{x}_t at an arbitrary time step t given \mathbf{x}_0 and \mathbf{y} by using the so-called *perturbation kernel*,

$$p_{0t}(\mathbf{x}_t | \mathbf{x}_0, \mathbf{y}) = \mathcal{N}_{\mathbb{C}}(\mathbf{x}_t; \boldsymbol{\mu}(\mathbf{x}_0, \mathbf{y}, t), \sigma(t)^2 \mathbf{I}), \quad (4)$$

where $\mathcal{N}_{\mathbb{C}}$ denotes the circularly-symmetric complex normal distribution and \mathbf{I} is the identity matrix. We utilize equations

(5.50, 5.53) in Särkkä & Solin [36] to determine closed-form solutions for the mean

$$\boldsymbol{\mu}(\mathbf{x}_0, \mathbf{y}, t) = e^{-\gamma t} \mathbf{x}_0 + (1 - e^{-\gamma t}) \mathbf{y}, \quad (5)$$

and the variance

$$\sigma(t)^2 = \frac{\sigma_{\min}^2 \left((\sigma_{\max}/\sigma_{\min})^{2t} - e^{-2\gamma t} \right) \log(\sigma_{\max}/\sigma_{\min})}{\gamma + \log(\sigma_{\max}/\sigma_{\min})}. \quad (6)$$

Vincent [31] shows that fitting the score model \mathbf{s}_θ to the score of the perturbation kernel $\nabla_{\mathbf{x}_t} \log p_{0t}(\mathbf{x}_t | \mathbf{x}_0, \mathbf{y})$ is equivalent to implicit and explicit score matching [27] under some regularity conditions. This technique is called *denoising score matching* and essentially results in estimating

$$\nabla_{\mathbf{x}_t} \log p_{0t}(\mathbf{x}_t | \mathbf{x}_0, \mathbf{y}) = \nabla_{\mathbf{x}_t} \log \left[|2\pi\sigma\mathbf{I}|^{-\frac{1}{2}} e^{-\frac{\|\mathbf{x}_t - \boldsymbol{\mu}\|_2^2}{2\sigma^2}} \right] \quad (7)$$

$$= \nabla_{\mathbf{x}_t} \log |2\pi\sigma(t)\mathbf{I}|^{-\frac{1}{2}} - \nabla_{\mathbf{x}_t} \frac{\|\mathbf{x}_t - \boldsymbol{\mu}(\mathbf{x}_0, \mathbf{y}, t)\|_2^2}{2\sigma(t)^2} \quad (8)$$

$$= -\frac{\mathbf{x}_t - \boldsymbol{\mu}(\mathbf{x}_0, \mathbf{y}, t)}{\sigma(t)^2}, \quad (9)$$

where for simplicity we derived the score for the real and imaginary part of the complex normal distribution in Eq. (4), assuming they are independently distributed and each follow a real-valued multivariate normal distribution. Note that Eq. (9) involves division by $\sigma(t)^2$, which has very small numerical values (including 0) around $t = 0$. To avoid undefined values and numerical instabilities, we thus introduce a small minimum process time t_ε , as done previously in the literature [28]. At each training step, the procedure can then be described as follows: 1) sample a random $t \sim \mathcal{U}[t_\varepsilon, T]$, 2) sample $(\mathbf{x}_0, \mathbf{y})$ from the dataset, 3) sample $\mathbf{z} \sim \mathcal{N}_{\mathbb{C}}(\mathbf{z}; 0, \mathbf{I})$, and 4) sample \mathbf{x}_t from Eq. (4) by effectively computing

$$\mathbf{x}_t = \boldsymbol{\mu}(\mathbf{x}_0, \mathbf{y}, t) + \sigma(t)\mathbf{z}. \quad (10)$$

After passing $(\mathbf{x}_t, \mathbf{y}, t)$ to the score model, the final loss is an unweighted L_2 loss between the model output and the score of the perturbation kernel. By substituting Eq. (10) into Eq. (9), the overall training objective becomes,

$$\arg \min_{\theta} \mathbb{E}_{t, (\mathbf{x}_0, \mathbf{y}), \mathbf{z}, \mathbf{x}_t | (\mathbf{x}_0, \mathbf{y})} \left\| \mathbf{s}_\theta(\mathbf{x}_t, \mathbf{y}, t) + \frac{\mathbf{z}}{\sigma(t)} \right\|_2^2, \quad (11)$$

where the expectation is approximated by sampling all random variables at each training step as described above. Note that due to the cancellation of $\boldsymbol{\mu}(\mathbf{x}_0, \mathbf{y}, t)$, the loss does not explicitly involve \mathbf{y} , only as an input to the score model, meaning that the score model is not tasked with estimating any portion of \mathbf{y} directly. Finally, the minimization is achieved by optimizing the parameters θ using stochastic gradient descent.

C. Inference / Reverse sampling

For inference, we assume that a trained score model \mathbf{s}_θ is given, that approximates the true score for all $t \in [0, T]$. We can then generate clean speech \mathbf{x}_0 conditioned on the noisy or reverberant speech \mathbf{y} by solving the plug-in reverse SDE

in Eq. (3). To determine the initial condition of the reverse process at $t = T$, we sample

$$\mathbf{x}_T \sim \mathcal{N}_{\mathbb{C}}(\mathbf{x}_T; \mathbf{y}, \sigma(T)^2 \mathbf{I}), \quad (12)$$

which is a strongly corrupted version of the noisy speech \mathbf{y} as illustrated in Fig. 1. The denoising process which solves the task of speech enhancement or dereverberation is then based on iterating through the reverse process starting at $t = T$ and ending at $t = 0$.

There exist several computational methods to find numerical solutions for SDEs, which are based on an approximation to discrete time steps. To this end, the interval $[0, T]$ is partitioned into N equal subintervals of width $\Delta t = T/N$, which approximates the continuous formulation into the discrete reverse process $\{\mathbf{x}_T, \mathbf{x}_{T-\Delta t}, \dots, \mathbf{x}_0\}$. A common single-step method for solving this discretization is the Euler-Maruyama method. In each iteration step, the method refers to a previous state of the process and utilizes the drift and the Brownian motion to determine the current state.

In this work, we employ so-called predictor-corrector (PC) samplers proposed by Song et al. [28], which combine single-step methods for solving the reverse SDE with numerical optimization approaches such as annealed Langevin Dynamics [26]. PC samplers consist of two parts, a predictor and a corrector. The predictor can be any single-step method that aims to solve the reverse process by iterating through the reverse SDE. After each iteration step of the predictor, the current state of the process is refined by the corrector. The correction is based on Markov chain Monte Carlo sampling and can be understood as a stochastic gradient ascent optimizer that adds at each iteration step a small amount of noise after taking a step in the direction of the estimated score. One possible intuition about the use of stochastic correctors is that they allow the process state to escape local minima by use of stochasticity. However, Karras et al. [37] have recently argued that stochasticity is only necessary in the reverse process to correct for numerical truncation errors of the predictor, a need that could be effectively circumvented by further improving the quality of the score model and predictor.

Another numerical way of approximating the reverse process is by solving the corresponding *probability flow ODE*,

$$d\mathbf{x}_t = [-\mathbf{f}(\mathbf{x}_t, \mathbf{y}) + g(t)^2 \mathbf{s}_\theta(\mathbf{x}_t, \mathbf{y}, t)] dt, \quad (13)$$

which is the associated *deterministic process* of the stochastic reverse SDE in Eq. (3). It can be shown that for each diffusion process there exists an ODE that describes the same marginal probability density $p_t(\mathbf{x}_t)$ [28]. Enhancing the noisy or reverberant mixture is then based on solving this ODE. We also evaluate and compare this class of solvers for our task, specifically employing the Runge-Kutta method of fourth order with an error estimator of fifth order [38].

D. Data representation

We represent our data in the complex-valued STFT domain. Therefore, we operate on spectrograms which are elements of $\mathbb{C}^{T \times F}$, where T denotes the number of time frames dependent on the audio length, and F represents the number of frequency

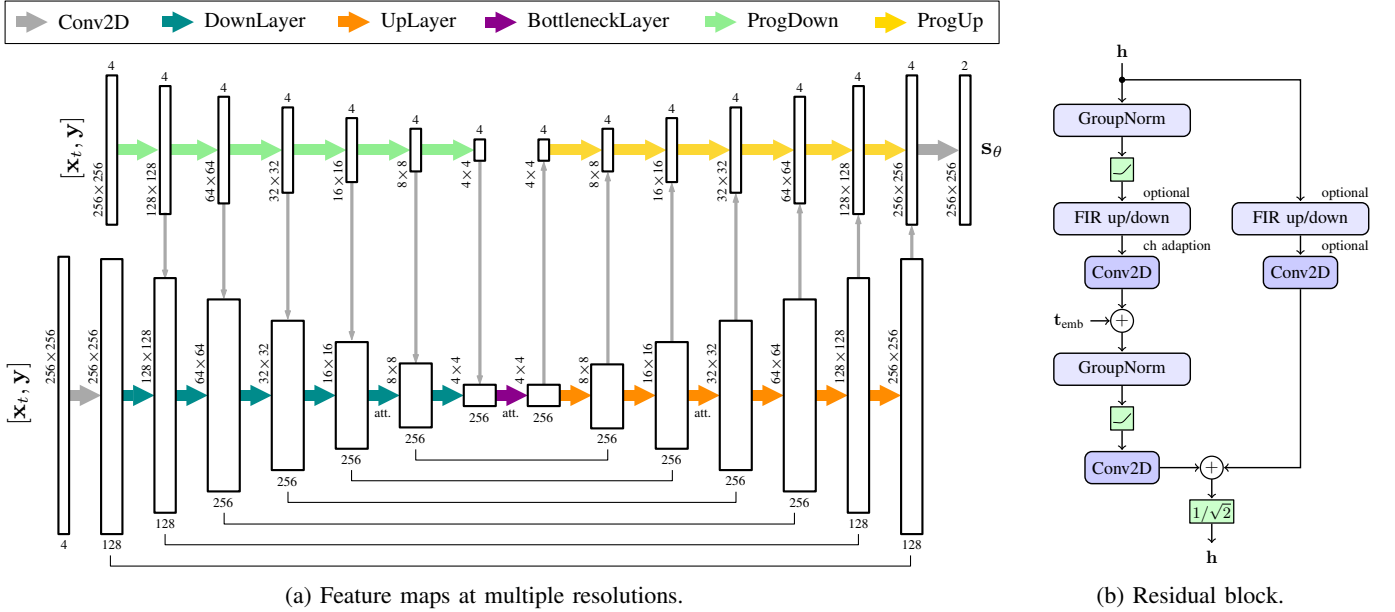


Fig. 3: NCSN++ network architecture used as a score model s_θ : The architecture is based on multi-resolution U-Net structure containing skip connections and an additional progressive growing path as shown in (a). Each up- and downsampling layer and the bottleneck layer consist of multiple residual blocks in series which are illustrated in (b).

bins. To be consistent with the description of the diffusion process above, we treat the spectrogram as a flattened vector in \mathbb{C}^d with $d = TF$.

Since the global distribution of STFT speech amplitudes is typically heavy-tailed [39], the information visible in untransformed spectrograms is dominated by only a small portion of time-frequency bins. Furthermore, the naturally encountered amplitudes often lie far outside the interval $[0, 1]$ often used in generative diffusion models, e.g., in the image domain [25], [28]. As an engineering trick, we thus apply an amplitude transformation

$$\tilde{c} = \beta |c|^\alpha e^{i\angle(c)} \quad (14)$$

to all complex STFT coefficients c , where $\angle(\cdot)$ represents the angle of a complex number. $\alpha \in (0, 1]$ is a compression exponent which brings out frequency components with lower energy (e.g. fricative sounds of unvoiced speech) [40], and $\beta \in \mathbb{R}_+$ is a simple scaling factor to normalize amplitudes roughly to within $[0, 1]$. The associated inverse transformation

$$c = \beta^{-1} |\tilde{c}|^{1/\alpha} e^{i\angle(\tilde{c})} \quad (15)$$

is applied before the signal is transformed back to the time-domain by using the inverse STFT.

III. NETWORK ARCHITECTURE

We utilize the *Noise Conditional Score Network* (NCSN++) architecture [28] for the score model s_θ and adapt it for the use of complex spectrograms. For this purpose, we consider the real and imaginary parts of the complex input as separate channels, since the original network only works with real-valued numbers. The network is based on a multi-resolution U-Net structure, which has been experimentally shown to be powerful for tasks such as generation and segmentation [41].

In Fig. 3a, we illustrate the architecture by showing the feature maps at each resolution, indicating their spatial dimension and the corresponding number of channels. The transformations between the feature maps are represented by arrows, where the color of the arrow specifies the type of transformation (see legend on top). Simple channel adaption is performed by using Conv2D layers with a kernel size of 3 and stride 1. Up- and downsampling layers are based on residual network blocks which are taken from the BigGAN architecture [42] and are shown in Fig. 3b. A residual block consist of Conv2D layers with same configuration as above, group normalization [43], up- or downsampling with finite impulse response (FIR) filters [44], and the Swish activation function [45]. Each upsampling layer consists of three residual blocks and each downsampling layer of two residual blocks in series with the last block performing the upsampling or downsampling. Global attention mechanisms [46] are added at a resolution of 16×16 and in the bottleneck layer to better learn global dependencies within the feature maps.

To make the model time-dependent, information about the current progression of the diffusion process is fed into the network architecture. A common practice is to use Fourier-embeddings [46], i.e., a learned projection that maps the scalar time coordinate t to an M -dimensional vector \mathbf{t}_{emb} that is integrated into every residual block as can be seen in Fig. 3b.

In addition to the main feature extraction path of the multi-resolution U-Net structure, the network incorporates a so-called progressive growing of the input which is seen at the top of Fig. 3a. The idea is to provide a downsampled version of the input to every feature map in the contracting path, which has been successful in stabilizing high-resolution image generation [47]. Note that the downsampling operation in the progressive growing use shared weights for each resolution.

TABLE I: Dataset information: Number of speakers, number of utterances, the total length for training and test (train / test), and the average length of an utterance in the test set.

Dataset	# speaker	# utterances	length [h]	len/ut [s]
WSJ0-CHiME3	101 / 8	12777 / 651	24.92 / 1.48	8.20
WSJ0-REVERB	101 / 8	12777 / 651	24.92 / 1.48	8.20
VB-DMD	28 / 2	11572 / 824	9.39 / 0.58	2.51

The same procedure is also used in the expansive path where a progressive growing of the output is informed by the feature maps at each resolution, resulting in the final score estimate.

IV. EXPERIMENTS

In this section, we describe the experimental setup for our speech enhancement and speech dereverberation experiments using the proposed method.

A. Datasets

For the evaluation of the speech enhancement task we use two datasets, the WSJ0-CHiME3 dataset and the VB-DMD dataset, which are described below. The use of two datasets allows cross evaluation, i.e. the test is performed on the other dataset than the training. The mismatched condition reveals information about how well the method generalizes to unseen data with different characteristics such as distinct noise types or different recording conditions. Moreover, to evaluate the performance of our approach on the dereverberation task, we create the WSJ0-REVERB dataset, which is also described below. Information about the number of speakers, number of utterances, and the total length of the train and test subset of each dataset can be found in Tab. I. We also report the average utterance length in the test set, which points to a limitation for VB-DMD because perceptual metrics such as PESQ or POLQA require a minimum length of 3.2s active speech [48].

a) WSJ0-CHiME3: We create the WSJ0-CHiME3 dataset using clean speech utterances from the Wall Street Journal (WSJ0) dataset [49] and noise signals from the CHiME3 dataset [50]. The mixture signal is created by randomly selecting a noise file and adding it to a clean utterance. Each utterance is used only once, and the SNR is sampled uniformly between 0 and 20 dB for training, validation, and test set.

b) VB-DMD: We use the publicly available VoiceBank-DEMAND dataset (VB-DMD) [51] which is often used as a benchmark for single-channel speech enhancement. The utterances are artificially contaminated with eight real-recorded noise samples from the DEMAND database [52] and two artificially generated noise samples (babble and speech shaped) at SNRs of 0, 5, 10, and 15 dB. The test utterances are mixed with different noise samples at SNR levels of 2.5, 7.5, 12.5, and 17.5 dB.

c) WSJ0-REVERB: To create the WSJ0-REVERB dataset, we use clean speech data from the WSJ0 dataset [49] and convolve each utterance with a simulated room impulse response (RIR). We use the `pyroomacoustics` engine [53] to simulate the RIRs. The reverberant room is modeled by sampling uniformly a T_{60} between 0.4 and 1.0 seconds. This

results in *measured* T_{60} between 0.4 and 1.8 seconds. A dry version of the room is generated with the same geometric parameters but a fixed absorption coefficient of 0.99, to generate the corresponding anechoic target. The resulting average direct-to-reverberant ratio (DRR) is around -9 dB.

B. Instrumental evaluation metrics

To evaluate the performance of the proposed method we use standard metrics which we will describe in detail below. All metrics employ full reference algorithms that rate the processed signal in relation to the clean reference signal using conventional digital signal analysis.

a) POLQA: The Perceptual Objective Listening Quality Analysis (POLQA) is an ITU-T standard that includes a perceptual model for predicting speech quality [54]. The POLQA score takes values from 1 (poor) to 5 (excellent) as usual for mean opinion scores (MOS).

b) PESQ: The Perceptual Evaluation of Speech Quality (PESQ) is used for objective speech quality testing and is standardized in ITU-T P.862 [55]. Although it is the predecessor of POLQA, it is still widely used in the research community. The PESQ score lies between 1 (poor) and 4.5 (excellent).

c) ESTOI: The Extended Short-Time Objective Intelligibility (ESTOI) is an instrumental measure for predicting intelligibility of speech subjected to various kinds of degradation [56]. The metric is normalized and lies between 0 and 1, with higher values indicating better intelligibility.

d) SI-SDR, SI-SIR, SI-SAR: Scale-Invariant (SI-) Signal-to-Distortion Ratio (SDR), Signal-to-Interference Ratio (SIR), and Signal-to-Artifact Ratio (SAR) are standard evaluation metrics for single-channel speech enhancement and speech separation [57]. They are all measured in dB, with higher values indicating better performance.

C. Listening Experiment

Instrumental evaluation metrics do not always correlate to subjective perception because there are many aspects of human perception that are very difficult to capture by computational means. Therefore, we conduct a MUSHRA listening experiment [58] with ten participants using the webMUSHRA framework [59]. The participants were asked to rate the overall quality of twelve randomly sampled examples from the WSJ0-CHiME3 test set as reconstructed by the compared algorithms. The results are reported on a quality scale from 0 to 100.

D. Hyperparameters and training configuration

a) Input representation: We convert each audio input into a complex-valued STFT representation using a window size of 510, resulting in $F = 256$, a hop length of 128 (i.e. approximately 75% overlap), and a periodic Hann window. To process multiple examples for batch training, the length of each spectrogram is trimmed to $T = 256$ STFT time frames, with start and end times selected randomly at each training step. For the spectrogram transformation in Eq. (14) and (15), we have chosen $\alpha = 0.5$ and $\beta = 0.15$ empirically.

TABLE II: Results for different sampler configurations tested on VB-DMD with the average number of function evaluations (NFE) and the respective average real-time factor (RTF)².

Type	Sampler settings	NFE	RTF	PESQ	SI-SDR [dB]
PC	0 corrector steps	30	0.89	2.80	15.38
PC	1 corrector steps	60	1.77	2.93	17.35
PC	2 corrector steps	90	2.65	2.92	17.52
ODE	atol=10 ⁻¹ , rtol=10 ⁻¹	14	0.46	2.78	12.83
ODE	atol=10 ⁻⁶ , rtol=10 ⁻³	49	1.55	2.71	12.76

b) *Stochastic process*: The SDE in Eq. (1) is parameterized with $\sigma_{\min} = 0.05$, $\sigma_{\max} = 0.5$ and $\gamma = 1.5$, where the stiffness γ is chosen such that the mean $\boldsymbol{\mu}$ in Eq. (5) is close to \mathbf{y} at $t = T$. We verify this assumption by demonstrating that $\mathbb{E}[\|\boldsymbol{\mu}(\mathbf{x}_0, \mathbf{y}, T) - \mathbf{y}\|^2] < 10^{-3}$, where the expectation calculated over all complex bins in a random sample of 256 spectrogram pairs from the chosen dataset. We set the minimum process time to $t_e = 0.03$.

c) *Training configuration*: We train the DNN on four Quadro RTX 6000 (24 GB memory each) for 160 epochs using the distributed data parallel (DDP) approach in PyTorch Lightning [60], which takes about one day. We use the Adam optimizer [61] with a learning rate of 10^{-4} and an effective batch size of $4 \times 8 = 32$. We track an exponential moving average of the DNN weights with a decay of 0.999, to be used for sampling [62]. We log the average PESQ value of 20 randomly chosen examples from the validation set during training and select the best-performing model for evaluation.

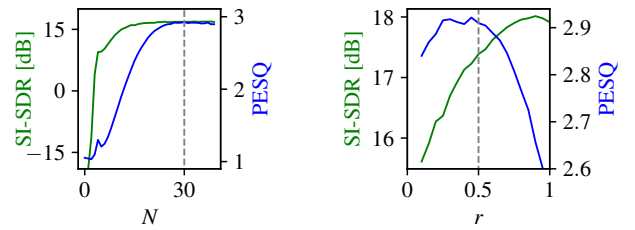
E. Sampler settings

To find optimal sampler settings for the reverse process, we run a hyperparameter search using the VB-DMD dataset.

a) *Sampler type*: We investigate which choice of sampler yields the best speech enhancement performance, comparing the PC sampler with different numbers of corrector steps and an ordinary ODE sampler as described in Sec. II-C. In Tab. II we can see that use of one correction step in the PC sampler seems to be advantageous, but the use of two steps does not lead to a further increase in performance. Thus, we decide to use the PC sampler with one corrector step for the evaluation. However, it should be noted that the use of one correction step doubles the number of function evaluations (NFE) of the sampler. The *function* being the expensive score model, this results in an average real-time factor (RTF) of 1.77, i.e., 1 sec of audio requires 1.77 sec of processing². Comparing the PC sampler with the ODE sampler, we find that the PC sampler performs better in both metrics. However, with suitable settings, the ODE sampler requires only 14 NFE on average which results in an improved RTF of only 0.46.

b) *Number of reverse steps N* : The number of reverse steps N can be used to set a balance between the computational effort and the performance of the model. In Fig. 4a, we show the speech enhancement performance as a function of N . It can be seen that SI-SDR starts to stagnate earlier than

²Average processing time for 10 audio files on an NVIDIA GeForce RTX 2080 Ti GPU, in a machine with an Intel Core i7-7800X CPU @ 3.50GHz.



(a) Varying N , fix $r = 0.33$

(b) Varying r , fix $N = 30$

Fig. 4: Model performance in PESQ and SI-SDR as a function of (a) the number of reverse steps N and (b) the step size parameter r in the annealed Langevin corrector.

PESQ. We opt for a value of $N = 30$, at which both metrics show no further increase in performance.

c) *Step size in corrector*: In Fig. 4b, we vary the step size r of the annealed Langevin dynamics in the corrector. Interestingly, this parameter represents a compromise between PESQ and SI-SDR. We choose $r = 0.5$ to achieve a maximum PESQ value while still obtaining a good value for SI-SDR.

F. Baselines

We compare the performance of our proposed method with four generative and four discriminative baselines which we describe in more detail below. All methods are re-trained by us, except for DVAE and MetricGAN+ on VB-DMD, for which we obtained the pretrained model from the authors who used the exact same training data.

a) *STCN [11]*: A generative VAE-based speech enhancement method which uses a stochastic temporal convolutional network (STCN) [63] that allows the latent variables to have both hierarchical and temporal dependencies. The parameters of the noise model and the latent variables are estimated using a Monte Carlo expectation maximization (MCEM) algorithm.

b) *DVAE [17]*: Generative speech enhancement method based on an unsupervised dynamical VAE (DVAE) [64] which models temporal dependencies between successive observable and latent variables. Parameters are updated at test time using a variational expectation maximization (VEM) method where the encoder is fine-tuned using stochastic gradient ascent.

c) *CDiffuSE [21]*: Most related to our proposed method is CDiffuSE, a generative speech enhancement method based on a conditional diffusion process defined in the time domain.

d) *SGMSE [22]*: Score-based Generative Model for Speech Enhancement (SGMSE) is our previous publication on which the proposed method is based. The main difference is that it uses a deep complex U-Net [65] instead of the NCSN++ architecture as the score model.

e) *MetricGAN+ [66]*: A discriminative speech enhancement method which uses a generator network for mask-based prediction of clean speech and introduces a discriminator network trained to approximate the PESQ score.

f) *Conv-TasNet [67]*: An end-to-end neural network that estimates a mask that is used for filtering a learned representation of the noisy mixture. The filtered representation is transformed back to the time domain by a learned decoder.

TABLE III: Speech enhancement results obtained for WSJ0-CHiME3 under matched and mismatched training conditions. Values indicate mean and standard deviation. Methods are sorted by the algorithm type, generative (G) or discriminative (D).

Method	Type	Training set	POLQA	PESQ	ESTOI	SI-SDR [dB]	SI-SIR [dB]	SI-SAR [dB]
Mixture	-	-	2.63 ± 0.67	1.70 ± 0.49	0.78 ± 0.14	10.0 ± 5.7	10.0 ± 5.7	-
STCN (MCEM) [11]	G	WSJ0	2.64 ± 0.68	2.01 ± 0.55	0.81 ± 0.12	13.5 ± 4.7	18.7 ± 5.5	15.4 ± 4.7
RVAE (VEM) [17]	G	WSJ0	2.97 ± 0.63	2.31 ± 0.55	0.85 ± 0.11	15.8 ± 5.0	21.6 ± 6.1	17.6 ± 4.9
CDiffuSE [21]	G	WSJ0-CHiME3	2.77 ± 0.52	2.15 ± 0.49	0.80 ± 0.09	7.3 ± 1.9	19.5 ± 6.0	7.8 ± 1.8
SGMSE [22]	G	WSJ0-CHiME3	2.98 ± 0.60	2.28 ± 0.57	0.86 ± 0.09	14.8 ± 4.3	25.4 ± 5.6	15.3 ± 4.2
SGMSE+	G	WSJ0-CHiME3	3.73 ± 0.53	2.96 ± 0.55	0.92 ± 0.06	18.3 ± 4.4	31.1 ± 4.6	18.6 ± 4.5
MetricGAN+ [66]	D	WSJ0-CHiME3	3.52 ± 0.61	3.03 ± 0.45	0.88 ± 0.08	10.5 ± 4.5	24.5 ± 5.1	10.7 ± 4.6
Conv-TasNet [67]	D	WSJ0-CHiME3	3.65 ± 0.54	2.99 ± 0.58	0.93 ± 0.05	19.9 ± 4.3	29.2 ± 4.6	20.6 ± 4.5
STCN (MCEM) [11]	G	VB	2.53 ± 0.66	1.80 ± 0.45	0.79 ± 0.12	11.9 ± 4.5	17.3 ± 4.9	13.8 ± 4.6
RVAE (VEM) [17]	G	VB	2.84 ± 0.61	2.08 ± 0.49	0.82 ± 0.11	13.9 ± 4.8	19.5 ± 5.9	15.8 ± 4.7
CDiffuSE [21]	G	VB-DMD	2.20 ± 0.50	1.84 ± 0.41	0.71 ± 0.10	3.8 ± 2.5	21.6 ± 7.0	4.0 ± 2.5
SGMSE [22]	G	VB-DMD	2.31 ± 0.44	1.62 ± 0.31	0.74 ± 0.11	10.5 ± 4.1	20.2 ± 7.6	11.4 ± 3.5
SGMSE+	G	VB-DMD	3.43 ± 0.61	2.48 ± 0.58	0.90 ± 0.07	16.2 ± 4.1	28.9 ± 4.6	16.4 ± 4.1
MetricGAN+ [66]	D	VB-DMD	2.47 ± 0.67	2.13 ± 0.53	0.76 ± 0.12	6.8 ± 3.1	22.9 ± 4.9	7.0 ± 3.1
Conv-TasNet [67]	D	VB-DMD	3.13 ± 0.60	2.40 ± 0.53	0.88 ± 0.08	15.2 ± 3.9	26.5 ± 4.6	15.6 ± 4.0

g) *GaGNet* [68]: This neural network is trained on a hybrid complex-domain and magnitude-domain regression objective for single-channel dereverberation. It uses so-called “glance” and “glaze” (GaG) modules, which respectively perform a coarse estimation of the magnitude and refine it with phase estimation in the complex domain.

h) *TCN+SA+S* [69]: This single-channel dereverberation approach uses a self-attention module to extract features from the input magnitude. This representation is then used by a temporal convolutional network followed by a single-layer convolutional smoother that outputs a magnitude estimate, which is used as the training objective. Griffin-Lim iterations are used to reconstruct the phase.

V. RESULTS

A. Speech Enhancement

In Tab. III, we report the speech enhancement results on the WSJ0-CHiME3 test set for the matched and mismatched condition, i.e. when the training set was also WSJ0-CHiME3 or when the training set was VB-DMD. We compare our proposed method, which we call *SGMSE+*, with selected baseline methods and sort the results by the type of algorithm, which is either generative or discriminative. Considering the matched condition in the upper half of Tab. III, we see that *SGMSE+* outperforms all other generative methods in all metrics, with bold values indicating the best method within the generative and discriminative methods, respectively. Note that STCN and RVAE are both unsupervised speech enhancement methods, i.e. they are trained on clean speech only (WSJ0 or VB). RVAE shows competitive results for SI-SAR, however, its VEM optimization algorithm is very time consuming due to the fine-tuning of the encoder at test time, resulting in a RTF of >10000 . This is significant in contrast to STCN with a RTF of 0.64 and *SGMSE+* with a RTF of 1.77². Although both VAE-based methods model temporal dependencies, they are limited in their ability to produce high quality speech, likely due to the dimensionality reduction of the latent variable and

the encoder’s sensitivity to noisy input, which causes the latent variable to be incorrectly initialized [15].

Comparing *SGMSE+* to our previous model *SGMSE*, we find a significant improvement, especially for the perceptual metrics. We report improvements of 0.75 for POLQA and 0.68 for PESQ. This shows that the proposed generative diffusion process benefits significantly from the increased model capacity of the NCSN++ architecture. In our previous paper [22], we have already shown improvements over *CDiffuSE* for *SGMSE* in SI-SDR and SI-SAR in the matched condition, which we now back up with also reporting slight improvements for the perceptual metrics. With *SGMSE+*, these improvements become even more significant with 0.96 improvement in POLQA and 11.0 dB in SI-SDR compared to *CDiffuSE*. In the qualitative analysis, we found that *SGMSE+* is more accurate than *CDiffuSE* in preserving the high frequencies of fricatives, which may be due to modeling the diffusion process in the T-F domain. In addition, unlike *CDiffuSE*, *SGMSE+* does not use the strategy of mixing some of the noisy mixture into the estimate, resulting in a significantly higher SI-SIR.

The comparison with *Conv-TasNet* and *MetricGAN+* shows that *SGMSE+* can keep up with the performance of discriminative methods and even surpasses them in terms of POLQA. However, for the matched condition, *MetricGAN+* achieves the best value for PESQ, which is likely due to the fact that the model is optimized for this metric. A similar behavior can be observed for *Conv-TasNet*, which achieves the highest value for SI-SDR, supposedly because the metric is also the loss function to be optimized during training. In contrast, this is not the case with *SGMSE+*, where the loss function does not contain any discriminative components and is only tasked with estimating the added white Gaussian noise.

Looking at the results for the mismatched condition in the bottom half of Tab. III, a general trend of decreasing metrics can be seen for all methods when comparing to the corresponding values of the matched condition. This was to be expected, since particular properties of the mismatched test set, such as distinct noise types or different recording

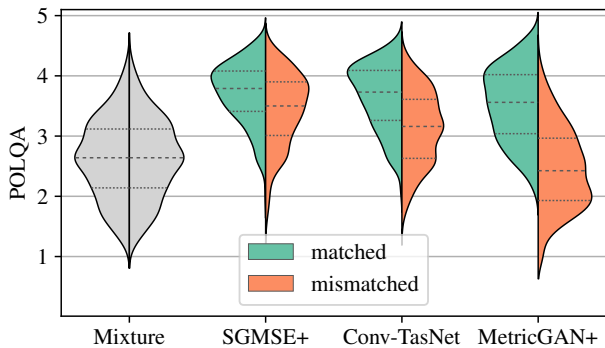


Fig. 5: Violin plots showing POLQA results for the matched and the mismatched condition with dashed and dotted lines representing median and quartiles, respectively.

characteristics of the clean speech have not been seen during training. However, generative methods generally show less degradation in the mismatched condition than discriminative methods. In particular, we see that SGMSE+ outperforms all other methods in all metrics under this condition, which shows the ability of our proposed method to generalize well.

Complementary to the average results above, we present in Fig. 5 violin plots of the full distribution of the POLQA scores obtained for SGMSE+, Conv-TasNet, MetricGAN+, and the noisy mixture for reference. For each method the distributions are plotted side by side for the matched and mismatched condition, so that the ability to generalize can be inferred from the horizontal alignment between both distributions. It can be seen that both distributions for SGMSE+ are relatively similar, whereas they are skewed for Conv-TasNet and especially for MetricGAN+.

In Fig. 6, we report the results of the subjective evaluation of the MUSHRA listening experiment in a boxplot. On average, the ten participants have rated the overall quality our proposed approach with the highest score. In addition, our method remains fairly robust when the model was trained on a different training set, while discriminative methods show much stronger degradation for the mismatched condition. Interestingly, MetricGAN+ was only rated with a median score less than 50 for the matched condition, although the method performed best among all baselines for PESQ (see Tab. III). This reveals the discrepancy between the use of instrumental metrics for evaluation and people’s actual perceptions. We suspect that MetricGAN+ has simply learned to utilize the internal operations of the PESQ algorithm to obtain a high value in this metric, neglecting the naturalness of the clean speech estimate. In fact, listening to the enhanced files, it can be recognized that the energy of the speech signal estimated by MetricGAN+ is mainly concentrated in the low- and mid-frequency area of the spectrogram, while high frequencies are strongly attenuated.

Listening to the enhanced files of our method, we notice that at very low input SNRs, some “vocalizing” artifacts with very poor articulation and no linguistic meaning are occasionally produced. In other examples, we find that breathing sounds or speech-like sounds were generated in noisy regions where no speech was originally present. These artifacts could also

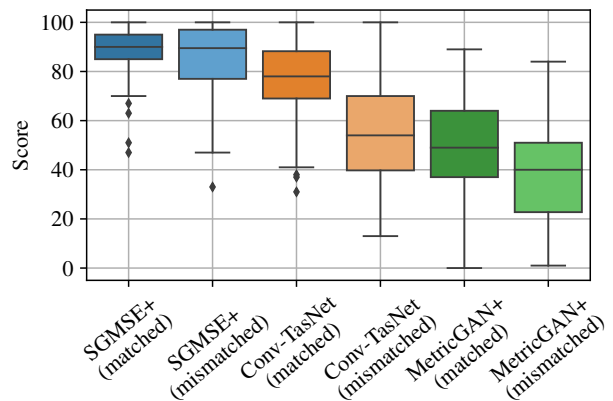


Fig. 6: Boxplot showing the results of the MUSHRA listening experiment with ten participants on twelve randomly selected examples.

TABLE IV: Speech enhancement results obtained for VB-DMD. Models marked with an asterisk (*) are additional baselines with values taken from the corresponding papers.

Method	Type	PESQ	ESTOI	SI-SDR [dB]
Mixture	-	1.97	0.79	8.4
SEGAN* [8]	G	2.16	-	-
RVAE [17]	G	2.43	0.79	16.4
MetricGAN-U* [70]	G	2.45	0.77	8.2
CDiffuSE [21]	G	2.46	0.79	12.6
SGMSE [22]	G	2.28	0.80	16.2
SGMSE+	G	2.93	0.87	17.3
UMX* [71]	D	2.35	0.83	14.0
Conv-TasNet [67]	D	2.84	0.85	19.1
MetricGAN+ [66]	D	3.13	0.83	8.5

explain the outliers of our method in the listening experiment (see Fig. 6). For the matched condition, for example, the two lowest outliers come from the same utterance with clearly noticeable vocalizing artifacts. We hypothesize that these artifacts can be linked to the generative nature of the proposed approach. Indeed, for very noisy inputs, the score model recognizes some energy in some time-frequency area and can erroneously identify it as some corrupted speech which needs enhancing. The reverse diffusion process therefore tries to produce speech where it did not originally exist. We argue that this behavior could be mitigated if some conditioning with respect to speech activity and phoneme identity would be added to the score model.

Finally, Tab. IV lists the results for the standardized VB-DMD dataset. This has the advantage that one can take values from other methods and copy them from the corresponding papers for a quick algorithmic comparison. Although most audio files in VB-DMD [51] are shorter than 3.2 sec and despite said required minimum length in the P.862.3 standard [48], the use of the PESQ measure seems to work for shorter files in this case and confirms the trend for evaluation on WSJ0+CHiME3. From Tab. IV, it can be seen that SGMSE+ outperforms all other generative baselines, and performs on par with the discriminative methods.

TABLE V: Single-channel dereverberation results obtained for WSJ0-REVERB test set. Values indicate mean and standard deviation. Methods are sorted by the algorithm type which is either generative (G) or discriminative (D).

Method	Type	POLQA	PESQ	ESTOI	SI-SDR	SI-SIR	SI-SAR
Mixture	-	1.76 ± 0.29	1.36 ± 0.19	0.46 ± 0.12	-7.3 ± 5.5	-7.5 ± 5.4	-
SGMSE [22]	G	1.79 ± 0.28	1.35 ± 0.15	0.57 ± 0.07	-7.4 ± 5.8	-1.1 ± 7.0	-6.2 ± 5.5
SGMSE+	G	3.24 ± 0.46	2.66 ± 0.48	0.84 ± 0.07	1.6 ± 7.8	9.4 ± 10.2	2.3 ± 7.2
Conv-TasNet [67]	D	2.41 ± 0.52	1.84 ± 0.42	0.73 ± 0.10	1.6 ± 5.3	12.1 ± 5.1	1.9 ± 5.4
TCN+SA+S [69]	D	2.92 ± 0.33	2.29 ± 0.36	0.79 ± 0.05	-4.4 ± 5.3	-2.3 ± 5.2	-0.6 ± 5.1
GaGNet [68]	D	2.62 ± 0.47	1.98 ± 0.46	0.73 ± 0.08	-0.6 ± 4.9	6.1 ± 3.9	0.4 ± 5.1

B. Dereverberation

We report in Tab. V the performance of our approach when trained and tested on a single-channel dereverberation task. We compare with SGMSE [22] and three discriminative baselines, namely Conv-TasNet [67], GaGNet [68] and TCN+SA+S [69].

Our proposed SGMSE+ approach performs particularly well in terms of instrumental metrics compared to all other baseline models. The low average input DRR of -9 dB constitutes a real challenge for discriminative approaches, which do not manage to separate the reverberation from the target without distorting the target signal, resulting in low quality scores. On the other hand, our approach benefits from generative modeling and is able to reconstruct speech with very high quality in most cases. This is, however, only true if the score is properly learned, which interestingly is not achieved by our previous SGMSE approach [22] which uses a complex U-Net as score model.

Furthermore, using the proposed approach SGMSE+ on a single-channel dereverberation task does not produce any of the vocalized artifacts observed in the speech enhancement experiments for low input SNRs. Although the reverberant signal is formally decorrelated in the time domain from the target by the randomness of reflections across the room, it still originates from the dry speech source. Therefore, we conjecture that the score model effectively detects whether the energy in a particular time-frequency area is associated with the clean speech nearby that needs to be reconstructed.

A complementary interpretation of this difference in behavior can be taken from the point of view of manifold learning, under which the two tasks are very different. In most denoising tasks, speech and noise distributions are rather orthogonal (which is a relative notion as strictly speaking these distributions lie on non-linear manifolds and not linear subspaces). In the dereverberation task, however, one could illustrate the reverberation process as browsing a manifold family parameterized by the T_{60} reverberation time, with rather smooth trajectories. The “clean” (anechoic) data manifold then corresponds to a minimal T_{60} , and is smoothly morphed toward a reverberant manifold by increasing the T_{60} . Thus, it is reasonable to use a diffusion model for the dereverberation problem, as the forward and reverse processes figuratively correspond to a trajectory along this smooth manifold family, browsed in one direction or the other.

VI. CONCLUSION

In this work, we built upon on our existing work [22] that uses a novel stochastic diffusion process to design a generative

model for speech enhancement in the complex STFT domain. We presented an extended theoretical analysis of the underlying score-based generative modeling and explored different sampling strategies to solve the reverse process at test time. By using an advanced network architecture that we adapted for complex spectrograms, we were able to significantly improve the performance compared to our previous model.

In the experiments, we evaluated the speech enhancement performance under matched and mismatched conditions, i.e. when the training and test data were taken from the same or different corpora. For the matched condition, the proposed generative speech enhancement method performs on par with state-of-the-art discriminative methods. For the mismatched condition, our method shows strong generalization capabilities and outperforms all baselines in all metrics, as confirmed by a subjective listening test. Furthermore, we evaluated the proposed method on the task of speech dereverberation and show significantly superior performance compared to discriminative baseline methods. This shows that our method, with an improved network architecture, can also be used to enhance speech signals with other distortion types.

ACKNOWLEDGMENTS

We would like to thank J. Berger and Rohde&Schwarz SwissQual AG for their support with POLQA.

REFERENCES

- [1] R. C. Hendriks, T. Gerkmann, and J. Jensen, *DFT-domain based single-microphone noise reduction for speech enhancement: A survey of the state-of-the-art*. Morgan & Claypool, 2013.
- [2] T. Gerkmann and E. Vincent, “Spectral masking and filtering,” in *Audio Source Separation and Speech Enhancement*, E. Vincent, T. Virtanen, and S. Gannot, Eds. John Wiley & Sons, 2018.
- [3] D. Wang and J. Chen, “Supervised speech separation based on deep learning: An overview,” *IEEE Trans. on Audio, Speech, and Language Proc. (TASLP)*, vol. 26, no. 10, pp. 1702–1726, 2018.
- [4] D. S. Williamson, Y. Wang, and D. Wang, “Complex ratio masking for monaural speech separation,” *IEEE Trans. on Audio, Speech, and Language Proc. (TASLP)*, vol. 24, no. 3, pp. 483–492, 2015.
- [5] S.-W. Fu, T.-Y. Hu, Y. Tsao, and X. Lu, “Complex spectrogram enhancement by convolutional neural network with multi-metrics learning,” *IEEE Int. Workshop on Machine Learning for Signal Proc. (MLSP)*, pp. 1–6, 2017.
- [6] S.-W. Fu, Y. Tsao, X. Lu, and H. Kawai, “Raw waveform-based speech enhancement by fully convolutional networks,” *IEEE Asia-Pacific Signal and Inf. Proc. Assoc. Annual Summit and Conf. (APSIPA ASC)*, 2017.
- [7] P. Wang, K. Tan, and D. L. Wang, “Bridging the gap between monaural speech enhancement and recognition with distortion-independent acoustic modeling,” *IEEE Trans. on Audio, Speech, and Language Proc. (TASLP)*, vol. 28, pp. 39–48, 2020.

- [8] S. Pascual, A. Bonafonte, and J. Serrà, “SEGAN: Speech enhancement generative adversarial network,” *ISCA Interspeech*, pp. 3642–3646, 2017.
- [9] Y. Bando, M. Mimura, K. Itoyama, K. Yoshii, and T. Kawahara, “Statistical speech enhancement based on probabilistic integration of variational autoencoder and non-negative matrix factorization,” *IEEE Int. Conf. on Acoustics, Speech and Signal Proc. (ICASSP)*, pp. 716–720, 2018.
- [10] S. Leglaive, L. Girin, and R. Horaud, “A variance modeling framework based on variational autoencoders for speech enhancement,” *IEEE Int. Workshop on Machine Learning for Signal Proc. (MLSP)*, pp. 1–6, 2018.
- [11] J. Richter, G. Carbajal, and T. Gerkmann, “Speech enhancement with stochastic temporal convolutional networks,” *ISCA Interspeech*, pp. 4516–4520, 2020.
- [12] G. Carbajal, J. Richter, and T. Gerkmann, “Guided variational autoencoder for speech enhancement with a supervised classifier,” *IEEE Int. Conf. on Acoustics, Speech and Signal Proc. (ICASSP)*, pp. 681–685, 2021.
- [13] —, “Disentanglement learning for variational autoencoders applied to audio-visual speech enhancement,” *IEEE Workshop on Applications of Signal Proc. to Audio and Acoustics (WASPAA)*, pp. 126–130, 2021.
- [14] Y. Bando, K. Sekiguchi, and K. Yoshii, “Adaptive neural speech enhancement with a denoising variational autoencoder,” *ISCA Interspeech*, pp. 2437–2441, 2020.
- [15] H. Fang, G. Carbajal, S. Wermter, and T. Gerkmann, “Variational autoencoder for speech enhancement with a noise-aware encoder,” *IEEE Int. Conf. on Acoustics, Speech and Signal Proc. (ICASSP)*, pp. 676–680, 2021.
- [16] A. A. Nugraha, K. Sekiguchi, and K. Yoshii, “A flow-based deep latent variable model for speech spectrogram modeling and enhancement,” *IEEE Trans. on Audio, Speech, and Language Proc. (TASLP)*, vol. 28, pp. 1104–1117, 2020.
- [17] X. Bie, S. Leglaive, X. Alameda-Pineda, and L. Girin, “Unsupervised speech enhancement using dynamical variational auto-encoders,” *arXiv preprint arXiv:2106.12271*, 2021.
- [18] D. P. Kingma and M. Welling, “Auto-encoding variational Bayes,” *Int. Conf. on Learning Representations (ICLR)*, 2014.
- [19] I. Goodfellow, J. Pouget-Abadie, M. Mirza, B. Xu, D. Warde-Farley, S. Ozair, A. Courville, and Y. Bengio, “Generative adversarial networks,” *Advances in Neural Inf. Proc. Systems (NeurIPS)*, vol. 27, 2014.
- [20] Y.-J. Lu, Y. Tsao, and S. Watanabe, “A study on speech enhancement based on diffusion probabilistic model,” *IEEE Asia-Pacific Signal and Inf. Proc. Assoc. Annual Summit and Conf. (APSIPA ASC)*.
- [21] Y.-J. Lu, Z.-Q. Wang, S. Watanabe, A. Richard, C. Yu, and Y. Tsao, “Conditional diffusion probabilistic model for speech enhancement,” *IEEE Int. Conf. on Acoustics, Speech and Signal Proc. (ICASSP)*, 2022.
- [22] S. Welker, J. Richter, and T. Gerkmann, “Speech enhancement with score-based generative models in the complex STFT domain,” *ISCA Interspeech*, 2022.
- [23] J. Serrà, S. Pascual, J. Pons, R. O. Araz, and D. Scaini, “Universal speech enhancement with score-based diffusion,” *arXiv preprint arXiv:2206.03065*, 2022.
- [24] J. Sohl-Dickstein, E. Weiss, N. Maheswaranathan, and S. Ganguli, “Deep unsupervised learning using nonequilibrium thermodynamics,” *Int. Conf. on Machine Learning (ICML)*, pp. 2256–2265, 2015.
- [25] J. Ho, A. Jain, and P. Abbeel, “Denoising diffusion probabilistic models,” *Advances in Neural Inf. Proc. Systems (NeurIPS)*, vol. 33, pp. 6840–6851, 2020.
- [26] Y. Song and S. Ermon, “Generative modeling by estimating gradients of the data distribution,” *Advances in Neural Inf. Proc. Systems (NeurIPS)*, vol. 32, 2019.
- [27] A. Hyvärinen and P. Dayan, “Estimation of non-normalized statistical models by score matching,” *Journal of Machine Learning Research*, vol. 6, no. 4, 2005.
- [28] Y. Song, J. Sohl-Dickstein, D. P. Kingma, A. Kumar, S. Ermon, and B. Poole, “Score-based generative modeling through stochastic differential equations,” *Int. Conf. on Learning Representations (ICLR)*, 2021.
- [29] B. D. Anderson, “Reverse-time diffusion equation models,” *Stochastic Processes and their Applications*, vol. 12, no. 3, pp. 313–326, 1982.
- [30] Y. Koizumi, H. Zen, K. Yatabe, N. Chen, and M. Bacchiani, “SpecGrad: Diffusion probabilistic model based neural vocoder with adaptive noise spectral shaping,” *ISCA Interspeech*, 2022.
- [31] P. Vincent, “A connection between score matching and denoising autoencoders,” *Neural Computation*, vol. 23, no. 7, pp. 1661–1674, 2011.
- [32] N. Chen, Y. Zhang, H. Zen, R. J. Weiss, M. Norouzi, and W. Chan, “WaveGrad: Estimating gradients for waveform generation,” *Int. Conf. on Learning Representations (ICLR)*, 2021.
- [33] G. Batzolis, J. Stanczuk, C.-B. Schönlieb, and C. Etmann, “Conditional image generation with score-based diffusion models,” *arXiv preprint arXiv:2111.13606*, 2021.
- [34] P. Dhariwal and A. Nichol, “Diffusion models beat GANs on image synthesis,” *Advances in Neural Inf. Proc. Systems (NeurIPS)*, vol. 34, 2021.
- [35] C.-W. Huang, J. H. Lim, and A. C. Courville, “A variational perspective on diffusion-based generative models and score matching,” *Advances in Neural Inf. Proc. Systems (NeurIPS)*, vol. 34, 2021.
- [36] S. Särkkä and A. Solin, *Applied Stochastic Differential Equations*. Cambridge University Press, 2019.
- [37] T. Karras, M. Aittala, T. Aila, and S. Laine, “Elucidating the design space of diffusion-based generative models,” *arXiv preprint arXiv:2206.00364*, 2022.
- [38] J. R. Dormand and P. J. Prince, “A family of embedded Runge-Kutta formulae,” *Journal of Computational and Applied Mathematics*, vol. 6, pp. 19–26, 1980.
- [39] T. Gerkmann and R. Martin, “Empirical distributions of DFT-domain speech coefficients based on estimated speech variances,” *Int. Workshop on Acoustic Echo and Noise Control*, 2010.
- [40] S. Braun and I. Tashev, “A consolidated view of loss functions for supervised deep learning-based speech enhancement,” *Int. Conf. on Telecom. and Signal Proc. (TSP)*, pp. 72–76, 2021.
- [41] O. Ronneberger, P. Fischer, and T. Brox, “U-net: Convolutional networks for biomedical image segmentation,” *Int. Conf. on Medical image computing and computer-assisted intervention*, pp. 234–241, 2015.
- [42] A. Brock, J. Donahue, and K. Simonyan, “Large scale GAN training for high fidelity natural image synthesis,” *Int. Conf. on Learning Representations (ICLR)*, 2018.
- [43] Y. Wu and K. He, “Group normalization,” *Proc. of the European conference on computer vision (ECCV)*, pp. 3–19, 2018.
- [44] R. Zhang, “Making convolutional networks shift-invariant again,” *Int. Conf. on Machine Learning (ICML)*, pp. 7324–7334, 2019.
- [45] P. Ramachandran, B. Zoph, and Q. V. Le, “Swish: a self-gated activation function,” *arXiv preprint arXiv:1710.05941*, 2017.
- [46] A. Vaswani, N. Shazeer, N. Parmar, J. Uszkoreit, L. Jones, A. N. Gomez, Ł. Kaiser, and I. Polosukhin, “Attention is all you need,” *Advances in Neural Inf. Proc. Systems (NeurIPS)*, 2017.
- [47] T. Karras, S. Laine, M. Aittala, J. Hellsten, J. Lehtinen, and T. Aila, “Analyzing and improving the image quality of StyleGAN,” *IEEE/CVF Conf. on Computer Vision and Pattern Recognition (CVPR)*, pp. 8110–8119, 2020.
- [48] ITU-T Rec. P.862.3, “Application guide for objective quality measurement based on Recommendations P.862, P.862.1 and P.862.2,” *Int. Telecom. Union (ITU)*, 2007.
- [49] J. S. Garofolo, D. Graff, D. Paul, and D. Pallett, “CSR-I (WSJ0) Complete.” [Online]. Available: <https://catalog.ldc.upenn.edu/LDC93S6A>
- [50] J. Barker, R. Marxer, E. Vincent, and S. Watanabe, “The third ‘CHiME’ speech separation and recognition challenge: Dataset, task and baselines,” *IEEE Workshop on Automatic Speech Recognition and Understanding (ASRU)*, pp. 504–511, 2015.
- [51] C. Valentini-Botinhao, X. Wang, S. Takaki, and J. Yamagishi, “Investigating RNN-based speech enhancement methods for noise-robust text-to-speech,” *ISCA Speech Synthesis Workshop (SSW)*, pp. 146–152, 2016.
- [52] J. Thiemann, N. Ito, and E. Vincent, “The Diverse Environments Multi-channel Acoustic Noise Database (DEMAND): A database of multi-channel environmental noise recordings,” *The Journal of the Acoustical Society of America*, vol. 133, no. 5, pp. 3591–3591, 2013.
- [53] R. Scheibler, E. Bezzam, and I. Dokmanic, “Pyroomacoustics: A python package for audio room simulation and array processing algorithms,” in *IEEE Int. Conf. on Acoustics, Speech and Signal Proc. (ICASSP)*, apr 2018.
- [54] ITU-T Rec. P.863, “Perceptual objective listening quality prediction,” *Int. Telecom. Union (ITU)*, 2018. [Online]. Available: <https://www.itu.int/rec/T-REC-P.863-201803-1/en>
- [55] A. Rix, J. Beerends, M. Hollier, and A. Hekstra, “Perceptual evaluation of speech quality (PESQ) - a new method for speech quality assessment of telephone networks and codecs,” *IEEE Int. Conf. on Acoustics, Speech and Signal Proc. (ICASSP)*, vol. 2, pp. 749–752, 2001.
- [56] J. Jensen and C. H. Taal, “An algorithm for predicting the intelligibility of speech masked by modulated noise maskers,” *IEEE Trans. on Audio, Speech, and Language Proc. (TASLP)*, vol. 24, no. 11, pp. 2009–2022, 2016.
- [57] J. Le Roux, S. Wisdom, H. Erdogan, and J. R. Hershey, “SDR-half-baked or well done?” *IEEE Int. Conf. on Acoustics, Speech and Signal Proc. (ICASSP)*, pp. 626–630, 2019.

- [58] ITU-R Rec. BS.1534-3, “Method for the subjective assessment of intermediate quality level of audio systems,” *Int. Telecom. Union (ITU)*, 2014.
- [59] M. Schoeffler, S. Bartoschek, F.-R. Stöter, M. Roess, S. Westphal, B. Edler, and J. Herre, “webmushra—a comprehensive framework for web-based listening tests,” *Journal of Open Research Software*, vol. 6, no. 1, 2018.
- [60] W. Falcon et al., “Pytorch lightning,” *GitHub: <https://github.com/PyTorchLightning/pytorch-lightning>*, vol. 3, 2019.
- [61] D. P. Kingma and J. Ba, “Adam: A method for stochastic optimization,” *Int. Conf. on Learning Representations (ICLR)*, 2015.
- [62] Y. Song and S. Ermon, “Improved techniques for training score-based generative models,” *Advances in Neural Inf. Proc. Systems (NeurIPS)*, vol. 33, pp. 12 438–12 448, 2020.
- [63] E. Aksan and O. Hilliges, “Stcn: Stochastic temporal convolutional networks,” *Int. Conf. on Learning Representations (ICLR)*, 2018.
- [64] L. Girin, S. Leglaive, X. Bie, J. Diard, T. Hueber, and X. Alameda-Pineda, “Dynamical variational autoencoders: A comprehensive review,” *Foundations and Trends in Machine Learning*, vol. 15, no. 1-2, pp. 1–175, 2021.
- [65] H.-S. Choi, J.-H. Kim, J. Huh, A. Kim, J.-W. Ha, and K. Lee, “Phase-aware Speech Enhancement with Deep Complex U-Net,” *arXiv preprint [arXiv:1903.03107](https://arxiv.org/abs/1903.03107)*, 2019.
- [66] S.-W. Fu, C. Yu, T.-A. Hsieh, P. Plantinga, M. Ravanelli, X. Lu, and Y. Tsao, “MetricGAN+: An improved version of MetricGAN for speech enhancement,” *arXiv preprint [arXiv:2104.03538](https://arxiv.org/abs/2104.03538)*, 2021.
- [67] Y. Luo and N. Mesgarani, “Conv-TasNet: Surpassing ideal time–frequency magnitude masking for speech separation,” *IEEE Trans. on Audio, Speech, and Language Proc. (TASLP)*, vol. 27, no. 8, pp. 1256–1266, 2019.
- [68] A. Li, C. Zheng, L. Zhang, and X. Li, “Glance and gaze: A collaborative learning framework for single-channel speech enhancement,” *Applied Acoustics*, vol. 187, p. 108499, 2022.
- [69] Y. Zhao, D. Wang, B. Xu, and T. Zhang, “Monaural speech dereverberation using temporal convolutional networks with self attention,” *IEEE Trans. on Audio, Speech, and Language Proc. (TASLP)*, vol. 28, pp. 1598–1607, 2020.
- [70] S.-W. Fu, C. Yu, K.-H. Hung, M. Ravanelli, and Y. Tsao, “MetricGAN-U: Unsupervised speech enhancement/dereverberation based only on noisy/reverberated speech,” *IEEE Int. Conf. on Acoustics, Speech and Signal Proc. (ICASSP)*, pp. 7412–7416, 2022.
- [71] S. Uhlich and Y. Mitsufuji, “Open-unmix for speech enhancement (UMX SE),” 2020. [Online]. Available: <https://github.com/sigsep/open-unmix-pytorch>